Kidney International, Vol. 52 (1997), pp. 1593–1601

VASCULAR BIOLOGY - HEMODYNAMICS - HYPERTENSION

Colocalization of demethylating enzymes and NOS and functional effects of methylarginines in rat kidney

AKIHIRO TOJO, WILLIAM J. WELCH, VIVIANE BREMER, MASUMI KIMOTO, KENJIRO KIMURA, MASAO OMATA, TADASHI OGAWA, PATRICK VALLANCE, and CHRISTOPHER S. WILCOX

The Second Department of Internal Medicine, University of Tokyo, Tokyo, and Department of Nutrition, The University of Tokushima, Tokushima, Japan; Division of Nephrology and Hypertension, Georgetown University Medical Center, Washington, D.C., USA; and Centre for Clinical Pharmacology, Department of Medicine, University College, London, London, United Kingdom

Colocalization of demethylating enzymes and NOS and functional effects of methylarginines in rat kidney. N^G-monomethylarginine (L-NMA) and asymmetric N^G, N^G-dimethylarginines (ADMA) are endogenous inhibitors of cellular L-arginine uptake and/or nitric oxide (NO) synthesis that are implicated in renal parenchymal and Dahl salt-sensitive hypertension. Since the L-arginine:(L-NMA+ADMA) ratio determines NO synthase (NOS) activity, we compared the immunohistochemical distribution of NOS with N^G, N^G-dimethylarginine dimethylaminohydrolase (DDAH), which inactivates dimethylarginines (DMA) and L-NMA by hydrolysis to L-citrulline. Neuronal NOS (nNOS) was expressed predominantly in tubular epithelial cells of macula densa (MD), endothelial NOS (eNOS) in vascular endothelial cells (EC), and inducible NOS (iNOS) quite widely in tubular epithelium, including proximal tubules (PT), thick ascending limbs of Henle (TAL), distal convoluted tubule and intercalated cells (IC) of the collecting duct. Immunostaining for DDAH was present in PT, TAL, MD, and IC, and was also present in the glomerulus, Bowman's capsule, and endothelium of blood vessels. DDAH was detected in small vesicles of TAL and PT by electron microscopic (EM) immunocytochemistry. To study the effects of methylarginines on tubuloglomerular feedback (TGF) response, vehicle or methylarginines (10^{-3} M) were added to artificial tubular fluid (ATF) perfused orthogradely from the late PT at 40 nl · min^{-1} while assessing changes in glomerular capillary pressure from proximal stop flow pressure (PSF). Whereas the maximal TGF responses were unchanged by vehicle (ΔTGF 0 ± 0%) or symmetric DMA (SDMA; +1 ± 2%, NS), they were enhanced by L-NMA (+22 ± 4%, $P < 0.001$) and asymmetric DMA (ADMA; +28 ± 3%, $P < 0.001$). Since L-arginine transport can regulate renal epithelial NO generation, methylarginines (10^{-3} M) or vehicle were co-perfused orthogradely with [^{3}H]-L-arginine from the late PT and collected at the early distal tubule to study arginine uptake from the perfused loop of Henle. All methylarginines reduced fractional loop [^{3}H] absorption significantly ($P < 0.001$; vehicle, 84 ± 6; ADMA, 49 ± 6; SDMA, 56 ± 6; L-NMA, 41 ± 6%). In conclusion, sites of DDAH expression in the vasculature or nephron are all sites of expression of an isoform of NOS. L-NMA, ADMA, and SDMA all inhibit renal tubular L-arginine uptake, whereas L-NMA and ADMA, but not SDMA, enhance TGF responses. Therefore, DDAH may regulate the cellular L-arginine: methylarginine levels in specific renal cells, thereby governing cell-specific L-arginine uptake and NO generation in renal tubular epithelium.

Key words: tubuloglomerular feedback, arginine transport, asymmetric dimethylarginine, symmetric dimethylarginine, monomethyl-L-arginine.

Received for publication March 17, 1997
and in revised form July 8, 1997
Accepted for publication July 10, 1997

Analogs of L-arginine such as N^G-monomethylarginine (L-NMA) and asymmetric N^G, N^G-dimethylarginine (ADMA), in which one of the guanidino nitrogens is methylated, are competitive inhibitors of NO synthase (NOS); the enantimetric form of ADMA, symmetric dimethylarginine (SDMA) is present in biological fluids in equimolar concentrations as ADMA but does not inhibit NOS [1–6]. Dimethylarginines (DMAs) are produced by endothelial cells in culture [5] and blood vessels [4], and are present in plasma and urine of rats and human subjects [1–3]. These data suggested that ADMA and perhaps L-NMA may be endogenous inhibitors of NOS *in vivo*. Indeed, ADMA inhibits the activity of endothelium-dependent relaxation of the aorta [1], saphenous vein [3] or cerebral blood vessels [6].

Recently, the enzyme N^G, N^G-dimethylarginine dimethylaminohydrolase (DDAH), which hydrolyzes DMA and L-NMA to L-citrulline, has been isolated in several tissues, including kidney, pancreas, liver, brain and aorta [7, 8]. DDAH could regulate the L-arginine-NO pathway by governing the degradation of endogenous inhibitors of NOS. In the normal rat kidney, both constitutive and inducible NOS isoforms are expressed in specific cell types [9–16]. Immunohistochemical techniques have located the constitutive, type I, neuronal NOS (nNOS) isoform in renal tubular epithelial cells of the macula densa (MD) [9–11, 15]. RT-PCR techniques have located mRNA for nNOS at several sites in the tubular epithelium, predominantly the inner medullary collecting ducts [16]. Using *in situ* hybridization techniques, mRNA for nNOS have been shown in macula densa [10, 15, 17]. A constitutive, type III, endothelial cell NOS (eNOS) isoform has been immunohistochemically in endothelial cells of renal vasculature [15, 18], and mRNA for eNOS have been demonstrated in renal vasculature and glomeruli by RT-PCR methods [12]. An inducible NOS (iNOS) has been located immunohistochemically in the intercalated cells of the collecting duct [13] and the afferent arterioles, thick ascending limb of Henle (TAL) and distal convoluted tubules of normal rats [11]. *In situ* hybridization methods [14] or RT-PCR applied to microdissected nephron segments [19] have located mRNA for iNOS in the glomerulus and several tubular sites, predominantly the collecting duct and TAL. These isoforms of NOS have been implicated in many functions of the normal kidney including regulation of the tubuloglomerular feedback (TGF) response [9], renal microcirculation [20], and salt [21] and proton transport [13].

The plasma concentrations of the DMA enantimers are increased in patients with chronic renal failure, and may contribute to the elevated blood pressure and pathophysiology of the uremic syndrome [1]. Moreover, renal excretion of ADMA is increased in Dahl salt-sensitive, compared to the salt-resistant rat fed a high-salt diet, and correlates with the level of blood pressure (BP) [22]. The intracellular concentration ratio of L-arginine:(L-NMA+ADMA) could be a regulatory factor in NO generation, and DDAH has a role in modulation of this ratio in the cell. However, the localization of DDAH in the kidney has not been studied. Therefore, the first aim of the present study was to investigate cellular and subcellular localization of DDAH in the normal rat kidney and compare this in the same study with the localization of different NOS isoforms.

The TGF response entails vasoconstriction of the afferent arteriole and a reduction in the glomerular capillary pressure and single-nephron glomerular filtration rate during delivery and reabsorption of NaCl at the macula densa segments [23]. This response is buffered by NO generation from nNOS in the MD [9, 24]. We have shown recently that macula densa NO generation is limited during salt restriction by L-arginine delivery and uptake from the lumen of the loop of Henle via system y^+ [25]. ADMA is a well-characterized inhibitor of NOS. In studies of endothelial cells in culture, ADMA, but not SDMA, inhibit NOS activity [1, 4], yet both enantimers inhibit L-arginine uptake by system y^+ [26]. Therefore, NO generation at the MD could be regulated not only by the rates of methylation and demethylation of L-arginine within cells, but also by luminal delivery of methylarginines, if they could compete with luminal L-arginine for system y^+ transport in the macula densa. Therefore, the second aim of the present study was to investigate the effects of ADMA, SDMA, and L-NMA on TGF and on the cellular [^{3}H]-L-arginine uptake from the perfused loop of Henle.

METHODS

Animal preparation

For the histochemical studies, 5 male Sprague-Dawley rats weighing 180 to 200 g were fed a standard rat chow (Na content 0.3 g · 100 g^{-1}) and given tap water to drink. An additional two rats were studied after receiving lipopolysaccharides (LPS; 4 mg · kg^{-1} i.p.) 20 and four hours before sacrifice to induce NOS in the kidney [19]. Rats were anesthetized with pentobarbital (50 mg · kg^{-1} i.p.). After cannulation of the abdominal aorta, the kidneys were perfused with phosphate buffered saline (PBS) followed by perfusion with periodate-lysine-paraformaldehyde (PLP) solution. Kidney slices for immunohistochemical studies were immersed in PLP overnight at 4°C. The tissue for light microscopic immunohistochemistry were embedded in wax (Polyethylene glycol 400 disterate; Polysciences Inc., Warrington, PA, USA), and that for immunogold studies was embedded in Lowicryl. The remaining tissue was processed for the pre-embedding immunoperoxidase method. These methods have been described in detail previously [11, 13, 27].

Light microscopic immunohistochemistry

The tissue was prepared as described in detail previously [11, 13, 27]. Wax sections (2 μm) were dewaxed, incubated first with 3% H_2O_2 to eliminate endogenous peroxidase activity, and thereafter with a monoclonal antibody directed against DDAH [7, 8] at a dilution of 1:1000 for 60 minutes after exposure to blocking serum. The monoclonal antibody to DDAH was raised against a 34 kD protein of DDAH extracted and purified from rat kidney [28]. Other sections were incubated with monoclonal antibodies against nNOS, eNOS, and iNOS at a dilution of 1:100 or a polyclonal antibody against iNOS (all from Transduction Laboratories, Lexington, KY, USA) at a dilution of 1:100. The sections were rinsed with Tris buffered saline containing 0.1% Tween 20 (TBST) and a biotinylated secondary antibody against mouse immunoglobulin (Dako, Glostrup, Denmark) for 20 minutes. Thereafter, sections were incubated with horseradish peroxidase (HRP)-conjugated streptavidin for 20 minutes. HRP labeling was detected by peroxidase substrate solution, diaminobenzidine (0.8 mM; Dojindo Laboratories, Kumamoto, Japan) and counterstained with hematoxylin before being examined under a light microscope.

Electron microscopic immunoperoxidase procedure

Sections (50 μm) of each kidney were cut on a vibratome, washed with 50 mM NH_4Cl in phosphate buffered saline, and incubated with 0.5% bovine serum albumin in TBST for 30 minutes, followed by incubation with the primary antibody against DDAH at 1:500 dilution overnight at 4°C. For a negative control, other sections were incubated without the antibody. After rinsing with TBST, the sections were incubated with a biotinylated secondary antibody directed against mouse immunoglobulin (Dako) for two hours and, after rinsing with TBST, were incubated with the HRP-conjugated streptavidin for one hour. The sections were rinsed and fixed with 1% glutaraldehyde in PBS for one hour, rinsed again, and HRP labeling was detected by peroxidase substrate solution, diaminobenzidine (0.8 mM; Dojindo Laboratories). The sections were postfixed in 2% osmium tetroxide in 0.1 M sodium cacodylate buffer for one hour at 4°C and embedded in epoxy resin. Sections (1 μm) were cut on an ultramicrotome and stained with toluidine blue for light microscopy. Ultrathin sections for electron microscopy were cut similarly, stained with lead citrate, and photographed on a transmission electron microscope (Hitachi H-7000; Hitachi, Tokyo, Japan).

Post-embedding immunogold procedure

One mm^3 blocks of cortical kidney tissue were embedded in Lowicryl. Ultrathin sections were mounted on colloidin-coated nickel grids and processed for immunogold labeling. The sections were incubated with 0.1 M NH_4Cl for one hour before rinsing with buffer solution (0.02 M Tris HCl, 0.15 M NaCl, 0.05% Tween 20, adjusted to pH 7.2) for 15 minutes. Primary mouse monoclonal antibody against DDAH, with 1:400 dilution, or eNOS (Transduction Laboratories), with 1:100 dilution, was applied and the sections were incubated overnight at 4°C. After washing them with buffer three times for 10 minutes, 30 nm gold-labeled goat anti-mouse IgG secondary antibody (Amersham Life Science, Buckinghamshire, UK) was applied to the sections for two hours in a dilution of 1:50. For double staining, the sections were rinsed with buffer and incubated with bovine serum for 15 minutes and the same process repeated with the other primary antibody and 15 nm immunogold particles. The sections were washed again with buffer (0.01 M PBS) and incubated with 2% glutaraldehyde/PBS solution for 30 minutes. Finally the sections were rinsed with distilled water, counterstained with uranyl acetate and lead citrate

and examined with an electron microscope (Hitachi-7000 transmission electron microscope).

Western blotting

The methods used have been described in detail previously [29, 30]. The right kidney was removed immediately before perfusion and fixation, flushed with ice-cold saline, and homogenized on ice with a Teflon glass tissue homogenizer (Iwaki, Chiba, Japan) in 1 ml buffer (pH 7.4) containing 50 mM Tris, 0.2 mM EDTA, 2 mM leupeptin, 50 mM DTT, 0.2 mM phenylmethylsulfonyl fluoride. Homogenates were centrifuged at 12,000 g for 20 minutes. The supernatants were diluted in sodium dodecyl sulfate (SDS) sample buffer (0.5 M Tris-HCl, 10% vol/vol glycerol, 10% wt/vol SDS, 5% vol/vol β-mercaptoethanol, 0.05% wt/vol bromphenol blue). Samples containing 600 μg protein were applied to 12.5% gel for DDAH and 7% gel for iNOS. Proteins were separated by SDS-PAGE, and electroblotted to nitrocellulose membrane that were incubated with 5% non-fat dry milk in TBST for one hour, following overnight incubation with a monoclonal antibody for DDAH at a 1:2000 dilution or with a monoclonal antibody for iNOS (Transduction Laboratories) at a 1:200 dilution. After rinsing in TBST, membranes were incubated for one hour with anti-mouse IgG antibody conjugated HRP at a 1:1000 dilution. After rinsing with TBST, blots were detected by diaminobenzidine with 0.3% hydrogen peroxide.

Microperfusion studies of [^{3}H]-L-arginine uptake from the lumen of the loop of Henle

To determine the effect of ADMA, SDMA, and L-NMA on TGF and L-arginine transport in the loop of Henle, male Sprague-Dawley rats (N = 20, wt 225 to 300 g) were prepared for renal micropuncture and microperfusion as described in detail previously [25, 31]. Rats were anesthetized with the thiobarbiturate, Inactin (100 mg · kg^{-1}; Research Biomedicals International, Natick, MA, USA). They received a standard chow (Ralston-Purina Co., St. Louis, MO, USA) with a Na^+ content of 0.3 g · 100 g^{-1}. The left kidney was immobilized and placed in a holding cup. The loop of Henle was microperfused with a glass micropipette (OD 10 to 12 μm) inserted into the last convolution of a superficial proximal tubule after placement of an immobile wax block proximal to the perfusion site.

For studies of TGF, 12 rats were prepared. An ultramicropipette (1 to 2 μm OD) was inserted into the proximal tubule (PT) upstream from the wax block. This pipette was connected to a servocontrolled pressure recorder (Instruments for Physiology and Medicine, La Jolla, CA, USA) to measure proximal stop flow (PSF) pressure. Changes in PSF reflect changes in glomerular capillary pressures. To activate TGF, the perfusion micropipette that was filled with artificial tubular fluid (ATF) was connected to a nanoliter perfusion pump (WPI, Sarasota, FL, USA) set to perfuse at 40 nl · min^{-1}. This provides maximal activation of TGF responses. To study the effects of luminal delivery of methylarginines on maximal TGF responses, PSF was measured during zero perfusion and while the nephron was perfused in random order with ATF + vehicle and ATF + L-NMA. Other nephrons were perfused to compare the response to ATF + vehicle with ATF + ADMA or ATF + vehicle with ATF + SDMA. All drugs were perfused at 10^{-3} M concentration. Maximal responses were achieved within 30 to 60 seconds of perfusion, were stable over 5 to 10 minutes of perfusion, and were reversible on cessation of perfusion.

For the studies of loop absorption of arginine, 8 rats were prepared, a nephron was selected, the PT blocked with wax at the midpoint, and the distal tubule (DT) identified. A perfusion micropipette was inserted into the last proximal convolution downstream from the wax block. Perfusion was set at 20 nl · min^{-1} using a calibrated nanoliter perfusion pump (WPI). Precisely timed collections of fluid were made from a second micropipette in the early distal tubule (EDT) at the surface of the kidney. Unidirectional L-arginine transport from the lumen of this nephron segment was studied by orthograde perfusion of the loop of Henle with ATF containing [^{3}H]-L-arginine (15 cpm · nl^{-1}; Amersham Life Sciences, Arlington Heights, IL, USA) and [^{14}C]-inulin (5 cpm · nl^{-1}; ICN, Costa Mesa, CA, USA) added as a recollection marker. The recovery of ^{3}H and ^{14}C were measured at the EDT collection site. In each case, the recollection of ^{14}C was 90 to 110% of the rate of delivery, indicating that there were no significant leaks. To evaluate the effects of ADMA, SDMA, and L-NMA on L-arginine transport from the lumen of the loop of Henle, ADMA, SDMA, and L-NMA (10^{-3} M; Sigma Chemical Co., St. Louis, MO, USA) or vehicle (0.154 M NaCl solution) were co-perfused with the artificial tubular fluid containing the radiochemical markers in random order through the test nephron. The collectate was transferred to a constant-bore capillary tube for measurement of tubular fluid volume prior to scintillation counting.

RESULTS

Light microscopy of DDAH in the kidney

Light microscopic observation of 2 μm wax sections demonstrated that there was strong immunostaining for DDAH in the endothelial cells of the arcuate (Fig. 1a) and renal arteries (Fig. 1b). Strong immunostaining for eNOS also was shown in the endothelial cells of the arcuate artery (Fig. 1c).

Immunostaining for DDAH was detected in the macula densa in some glomeruli and also in other cells in the glomerulus and Bowman's capsule (Fig. 2a). nNOS was present in macula densa cells and, as reported previously [11], there was also immunostaining for nNOS in Bowman's capsule cells in some glomeruli (Fig. 2b). DDAH immunoreactivity was also detected in the apical regions of the proximal convoluted tubules (PCT; Fig. 3a) and the cytoplasm of proximal straight tubules (PST; Fig. 3b) of the renal cortex. In the outer medulla, DDAH immunoreactivity was present in the TAL and in the intercalated cells of the cortical collecting duct (CCD; Fig. 4a). In the inner medulla, there was no significant labeling of DDAH, except for some staining in intercalated cells and endothelium of vasa recta (Fig. 4b). Light microscopic examination of the 1 μm Epon-sections showed immunostaining of the apical region of the PCT and intercalated cells of the CCD (Fig. 5a). The iNOS immunoreactivity, using a polyclonal antibody, was seen in the intercalated cells (Fig. 5b); TAL, PST, and vascular smooth muscle (data not shown). Using monoclonal antibodies for iNOS, there was no significant staining except for TAL (data not shown). The negative controls showed no staining of any structures in the kidney. The localization of DDAH and NOS isoforms are summarized in Table 1.

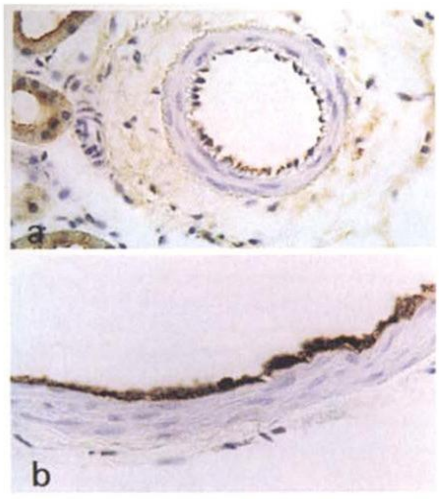

Figure 1

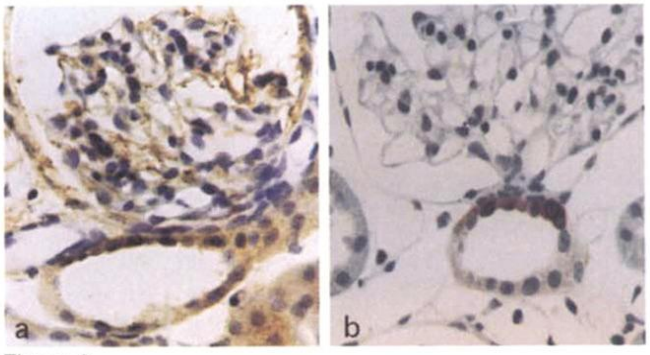

Figure 2

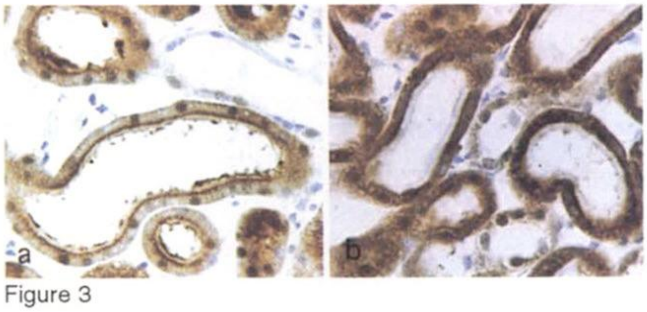

Figure 3

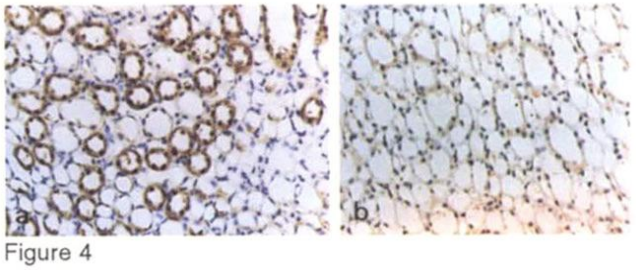

Figure 4

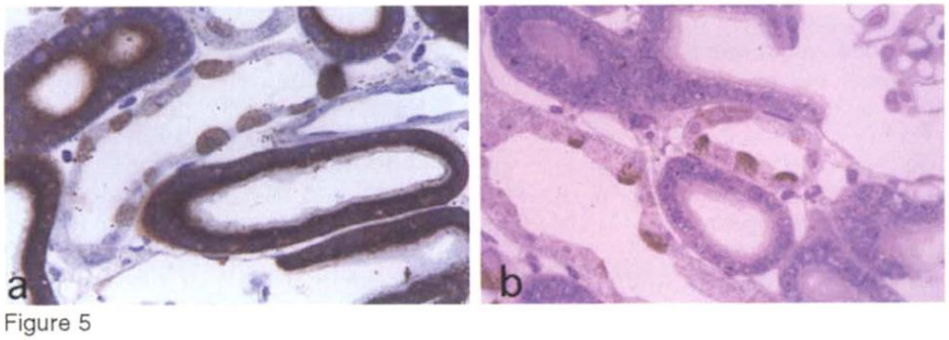

Figure 5

Fig. 1. Light micrograph illustrating immunostaining for DDAH in the arcuate artery (*a*), renal artery (*b*), and immunostaining for eNOS in the arcuate artery (*c*). Both DDAH and eNOS are strongly expressed in the endothelial cells of the renal vasculature. Magnification ×200.

Fig. 2. Light micrographs illustrating immunostaining for DDAH (*a*) and nNOS (*b*). Immunostaining for DDAH is observed in macula densa, glomerular and Bowman's capsular cells and, for nNOS, in macula densa cells. Magnification ×200.

Fig. 3. Light micrographs illustrating immunostaining for DDAH in proximal convoluted tubules (PCT; *a*) and proximal straight tubules (PST; *b*). Immunostaining for DDAH is detected in the apical region of PCT cells and is diffusely expressed in the cytoplasm of PST cells. Magnification ×170.

Fig. 4. Light micrographs illustrating immunostaining for DDAH in the outer medulla (*a*) and inner medulla (*b*). Immunostaining for DDAH is detected in cells of the thick ascending limb of the loop of Henle in the outer medulla, but there is no significant staining in the inner medulla. Magnification ×70.

Fig. 5. Light micrographs from 1 μm sections of a pre-embedding EM sample illustrating immunostaining for DDAH (*a*) and iNOS (*b*). Immunostaining for DDAH is located in the apical regions of both the proximal convoluted tubules and intercalated cells of the cortical collecting duct, whereas iNOS is expressed only in the intercalated cells. Magnification ×180.

Table 1. Immunostaining for DDAH and NOS isoforms in normal rat kidney

	DDAH	nNOS	eNOS	iNOS	
				Monoclonal Ab	Polyclonal Ab
Bowman's capsule	+	+	0	0	0
Glomerulus	+	0	+	0	0
PCT	+	0	0	0	+
PST	+	0	0	0	+
TAL	+	0	0	+	+
MD	+	+	0	0	0
DCT	0	0	0	0	+
CCD	+	0	0	0	+
OMCD	0	0	0	0	+
IMCD	0	+	0	0	+
Vessel					
Endothelium	+	0	+	0	0
SMC	0	0	0	0	+

Abbreviations are: Ab, antibody; PCT, proximal convoluted tubule; PST, proximal straight tubule; TAL, thick ascending limb of loop of Henle; DCT, distal convoluted tubule; CCD, cortical collecting duct; OMCD, outer medullary collecting duct; IMCD, inner medullary collecting duct; SMC, smooth muscle cell; +, immunostaining present; 0, immunostaining absent.

Electron microscopic distribution of DDAH

When examined by electron microscopy using the pre-embedding method, DDAH was detected in apical vesicles of the PCT (Fig. 6A) and in small vesicles through the cytoplasm of the TAL (Fig. 6B). There was no staining in the brush border membrane of the proximal tubule, mitochondria, and nuclei. Type A intercalated cells of the collecting duct showed some immunoreactivity, whereas adjacent principal cells were not stained (Fig. 6C). Type B cells also showed some immunoreactivity for DDAH (Fig. 6D). The immunogold method reconfirmed localization both DDAH and eNOS in glomerular endothelial cells (Fig. 7). Double staining was attempted with two different sizes of immunogold particles to determine whether DDAH and eNOS were colocalized. This demonstrated that both were expressed in the cytoplasm of glomerular endothelial cells (Fig. 7c).

Protein expression for DDAH and iNOS

Western blotting was used to detect DDAH and iNOS protein expressed in homogenates of kidneys from normal rats and rats stimulated with LPS. The antibody for DDAH produced a single band that corresponds to the DDAH protein with a molecular weight of 34 kDa. The kidney of LPS-injected rats demonstrated a band for DDAH with a similar density as seen in the normal rat, indicating that DDAH was not induced by LPS (Fig. 8). In contrast, Western blotting for iNOS did not detect a protein band in kidneys from normal rats but clearly detected a band corresponding to iNOS with a molecular weight of 130 kDa in the kidney after induction by LPS (Fig. 8).

Effects of methylarginines on TGF

As shown in Figure 9, rats had a strong maximal TGF response when tested by orthograde microperfusion of ATF into the loop of Henle at 40 nl · min^{-1} that did not differ between groups. Addition of vehicle to ATF did not modify the response. Likewise, the response was not altered by SDMA (ΔPSF before, 7.2 ± 0.4 vs. SDMA, 7.2 ± 0.4 mm Hg; $N = 6$; NS). However, L-NMA or ADMA both increase the response significantly (ΔPSF before, 8.3 ± 0.7 vs. L-NMA, 10.3 ± 1.1 mm Hg; $N = 6$; $P < 0.01$; before, 7.7 ± 0.4 vs. ADMA, 9.8 ± 0.5 mm Hg; $N = 7$; $P < 0.01$).

Effect of DMA and L-NMA on L-arginine transport

As shown in Figure 10, much of the [^{3}H]-L-arginine microperfused with ATF + vehicle from the late PT was reabsorbed from the loop of Henle by the EDT (84 ± 6%). Addition of L-NMA, ADMA or SDMA all reduced the fractional loop [^{3}H]-L-arginine reabsorption significantly ($P < 0.01$). Fractional reabsorption averaged 41 ± 6% with L-NMA, 49 ± 6% with ADMA, and 56 ± 5% with SDMA. These values did not differ significantly between the methylarginine derivatives.

Table 2 contains a comparison of the effects of the methylarginine derivatives on TGF and [^{3}H]-L-arginine absorption from the perfused loop of Henle. It is apparent that ADMA is as effective as L-NMA in both test systems, yet SDMA is effective only in preventing L-arginine uptake.

DISCUSSION

The main new findings from the present study are that sites of localization of DDAH correspond with sites of localization of NOS isoforms in the normal rat kidney. Unlike iNOS, DDAH is not strongly induced by LPS. Both ADMA and L-NMA enhance maximal TGF responses when microperfused luminally into the macula densa, whereas SDMA is ineffective. In contrast, all three methylarginine derivatives inhibit [^{3}H]-L-arginine uptake from the perfused loop of Henle to a similar degree.

Strong immunoreactivity for DDAH was observed in the endothelial cells of renal vasculature, including the main renal and arcuate arteries where eNOS was also shown clearly by light microscopic immunohistochemistry as in previous studies [15, 18, 30]. Using the EM immunogold method, DDAH and ecNOS were both located in glomerular endothelial cells. Immunocytochemical expression of eNOS in small renal vessels was clearly seen in this study. Therefore, DDAH and eNOS share common cell types of expression in the renal vascular endothelium.

Strong and uniform immunoreactive staining for nNOS was detected in the population of macula densa cells as in previous studies [9–11, 15, 27]. There was immunostaining in these cells also for DDAH, but, unlike nNOS, it was variable, and some macula densa cells were not stained with the antibody for DDAH.

There was staining of the intercalated cells of the cortical collecting duct with the polyclonal antibody to iNOS, as in previous studies [13]. This was also a site for immunostaining for DDAH. There was also staining for iNOS with the polyclonal antibody in the TAL and collecting ducts of the normal rat, corresponding to sites of iNOS immunoreactivity [13] or mRNA expression [14, 19] shown previously. In the present study, DDAH was also expressed at these sites.

The sites of expression of DDAH and NOS are compared in Table 1. It is apparent that all sites of immunoexpression for DDAH are also sites for expression of one of the NOS isoforms (Table 1). The only exception is that, whereas all cells of the macula densa stain uniformly and strongly for nNOS, immunostaining at this site for DDAH is more variable and some cells appear negative. It is not clear whether this represents a technical problem of DDAH antibody interaction with macula densa DDAH antigen or a genuine cell-to-cell variability in DDAH expression. The concurrence in immunoreactive staining cannot

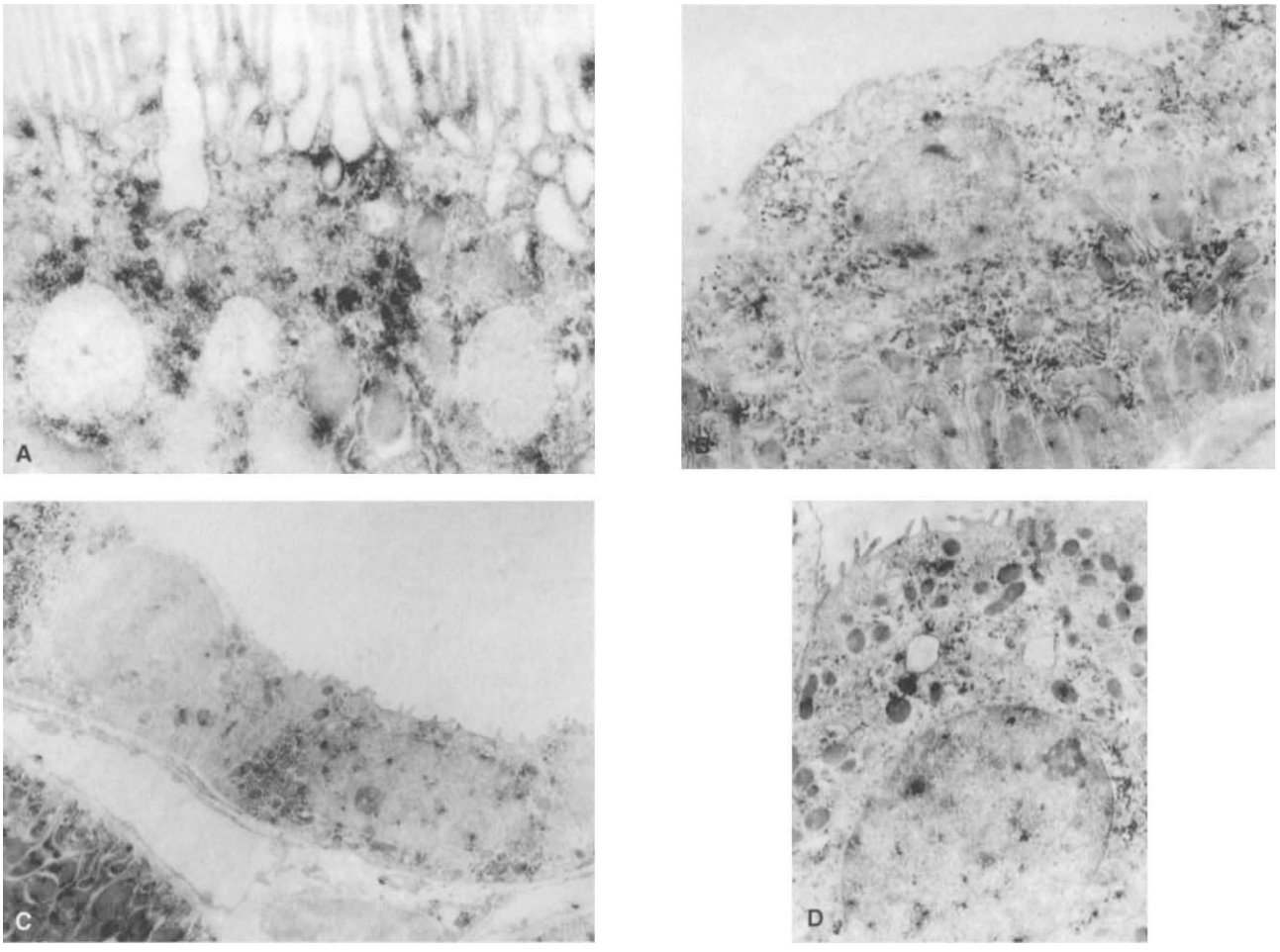

Fig. 6. Electron micrograph illustrating DDAH immunostaining using pre-embedding method in PCT (*A*), TAL (*B*), type A intercalated cells in the cortical collecting duct (CCD; *C*), and type B intercalated cells in the CCD (*D*) from normal rat kidney. Magnification: (A) ×18,000; (B) ×10,000; (C) ×4,500; (D) ×6,000.

be ascribed to cross-reactivity of the antibody because, as shown in Western analysis, DDAH antibodies recognize a single antigen at a molecular weight that corresponded to that of DDAH but not to any of the NOS isoforms.

The proximal tubule was a second site at which immunostaining for DDAH was not matched by staining for NOS. DDAH was strongly expressed in the apical region of PCT and in the cytoplasm of the PST, whereas there was rather inconsistent immunostaining for iNOS isoform of these cells under normal conditions. However, the proximal tubule is a site of NO generation. Thus, inhibition of NOS decreases NaCl and fluid reabsorption from superficial proximal convoluted tubule of the rat [32], or, in contrast, NO inhibits Na^+/H^+ exchanger in rabbit proximal tubules [33] and also inhibits Na^+,K^+-ATPase in proximal tubule cells cultured from the mouse [34]. These data suggest that endogenous NO inhibits Na^+ reabsorption in proximal tubules. LLC-PK_1 cells of proximal tubule origin express a functional NOS [35, 36], and iNOS can be induced plentifully in PCT cells in culture [37]. Moreover, mRNA for iNOS [19] and eNOS [12, 16] can be detected by RT-PCR techniques in microdissected proximal tubules. Therefore, although not detected consistently by immunohistochemical methods in this study, NOS is apparently expressed with DDAH in proximal tubular epithelium.

Western analysis of whole-kidney homogenates confirmed that LPS induced iNOS strongly [19]. Functional expression of iNOS following stimulation by LPS has been shown in mesangial cells [38] and proximal tubule and inner medullary collecting duct cells [39, 40]. In contrast, the LPS challenge did not appear to induce DDAH expression. The difference in response to LPS between DDAH and iNOS suggests that these two enzymes have distinct regulatory pathways.

The normal plasma level of ADMA and SDMA are about 1 μM [1]. This level of ADMA alone is probably not sufficient to inhibit NOS significantly. However, the concentrations of ADMA and SDMA increase substantially in the plasma of patients with uremia [1]. Moreover, these concentrations may well be much higher within certain cells since methylarginines are substrates for system y^+ transport into vascular endothelial and macrophage cells [26] and should thereby be concentrated intracellularly in cells that possess this transport characteristic. A system y^+ transport process has been located in blood vessels, vascular endothelial cells [26], macrophages [26, 41], and neuronal cells

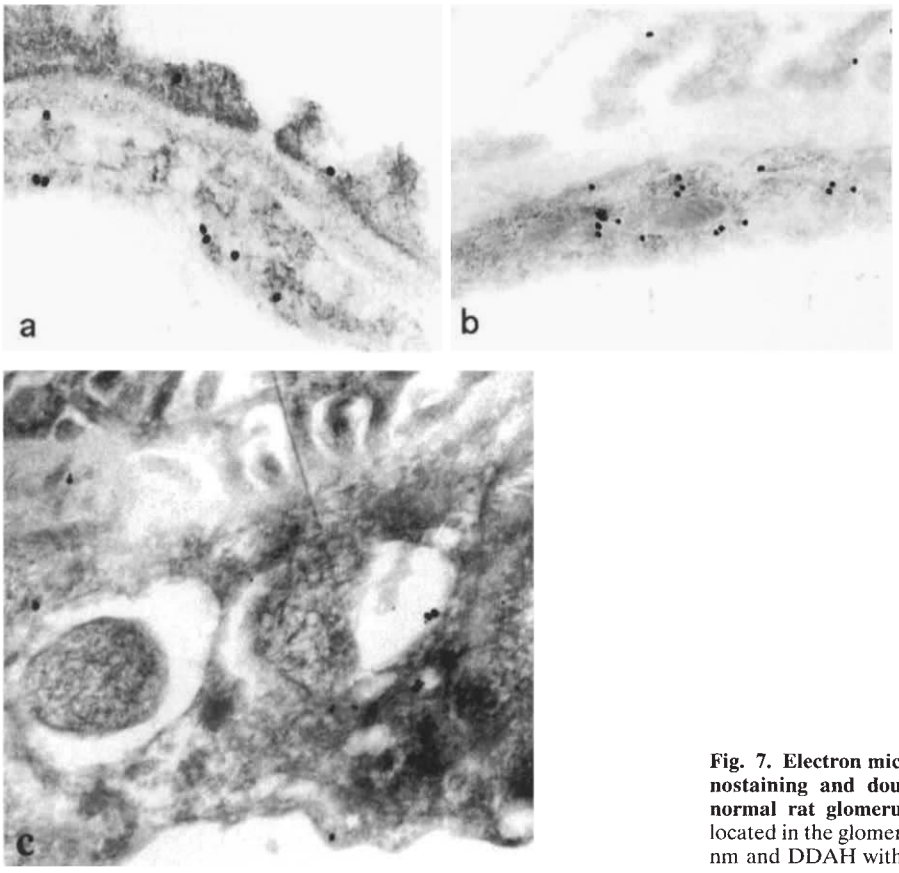

Fig. 7. Electron micrograph illustrating DDAH (*a*) and eNOS (*b*) immunostaining and double staining (*c*) with the immunogold method in normal rat glomeruli. Immunogold labeling for DDAH and eNOS is located in the glomerular endothelium. In panel c, eNOS is labeled with 30 nm and DDAH with 15 nm immunogold. Magnification ×26,000.

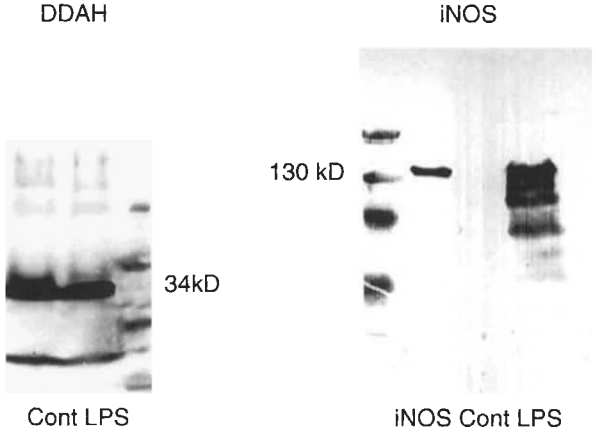

Fig. 8. Western blotting studies of DDAH and iNOS expression in the kidneys of the normal and LPS-injected rat. A strong band for DDAH is shown at 34 kDa in normal rat kidney, but it is not apparently induced by LPS treatment. A strong band for iNOS is seen at 130 kDa in kidneys from LPS-treated rats but is not seen in kidneys from normal rats. Molecular weight markers are shown.

[42] as well as the loop of Henle of the rat kidney [25, 43]. At these sites, cellular uptake of monomethyl- and dimethylarginine should be enhanced. SDMA, in addition to ADMA and L-NMA, are all substrates for y^+ transport at vascular endothelial cells, where they compete with arginine and other cationic amino acids for cellular uptake [26]. This consistent with the present finding that these three methylarginine derivatives were equally potent inhibitors of [^{3}H]-L-arginine uptake from the perfused loop of Henle.

We have shown previously that NO formed from NOS in the juxtaglomerular apparatus blunts expression of the TGF responses of normal or salt-replete rats [9, 24]. Recently, we found that microperfusion of L-arginine into the lumen of the macula densa blunts the TGF responses of normal or salt-depleted rats [25]. This effect depends on uptake of L-arginine via system y^+ since it is prevented by co-perfusion with an excess of the competing amino acid, L-lysine. It also depends on NOS since the response to arginine is stereospecific and is prevented by L-NMA. Thus, in salt-depleted rats, macula densa NO generation can be limited by L-arginine availability and cellular uptake. Where the intracellular levels of L-arginine can be below those required for maximum rates of NO generation from NOS, as at the macula densa, DDAH could be especially important in regulating NO generation. NOS activity at these sites should be a function of the intracellular ratio of L-arginine: (L-NMA + ADMA). Therefore, the co-localization of DDAH and NOS at several sites in the kidney is of interest, since it implies that these two regulatory enzymes could interact to set the level of NO generation at these segments. However, the details of this potential interaction between L-arginine and methylarginines has not yet been explored. It is uncertain whether ADMA within cells could inhibit L-arginine uptake via a *trans* effect.

The hypothesis that the L-arginine:methylarginine ratio can regulate NO generation *in vivo* has been tested recently in the

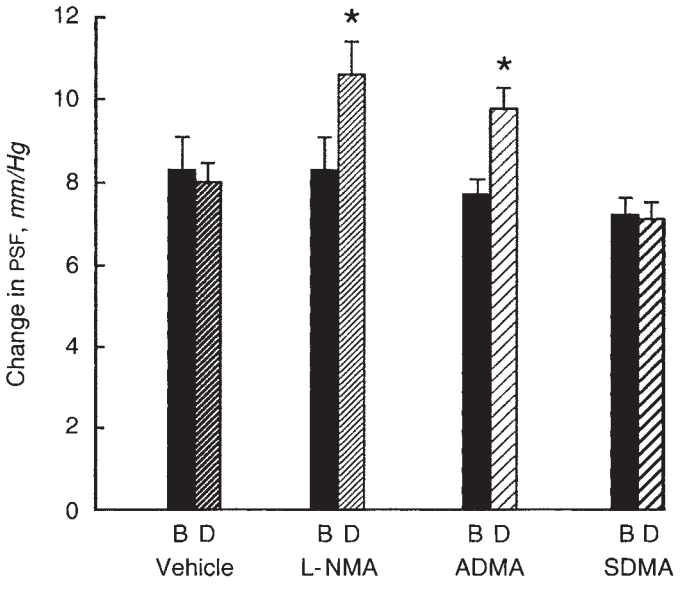

Fig. 9. Effect of methylarginines on maximal TGF responses. Mean ± SEM values for maximal TGF responses, assessed from changes in proximal stop flow pressure during increases in ATF perfusion from zero to 40 nl · min^{-1}. Data are shown before (B) and during (D) addition to ATF of vehicle (N = 10), L-NMA (N = 5), ADMA (N = 7), and SDMA (N = 6). N = number of nephrons. Compared to before: *$P < 0.01$.

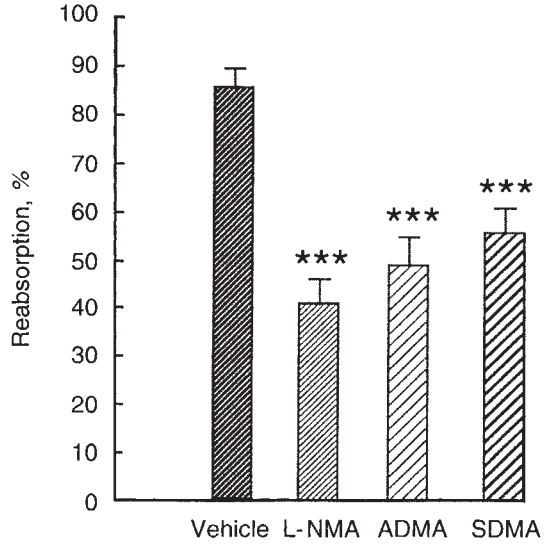

Fig. 10. Effect of methylarginines on loop of Henle reabsorption of L-arginine. Mean ± SEM values for percentage uptake of [^{3}H]-L-arginine from the perfused loop of Henle. The loop was perfused orthogradely with ATF + vehicle (N = 10), + L-NMA (N = 5), + ADMA (N = 10), or + SDMA (N = 12). N = number of nephrons. Compared to before: ***$P < 0.001$.

hypercholesterolemic rabbit [44], which has elevated plasma levels of ADMA and depressed levels of excretion of the NO metabolites, NO_2 + NO_3. L-arginine administration reversed the depressed L-arginine:methylarginine ratio and increases, but does not normalize, the excretion of NO metabolites [44].

We have previously reported that NO generation in interca-

Table 2. Effects of methylarginines on potentiation of maximal TGF responses or inhibition of labeled arginine uptake from the perfused loop of Henle

Addition to artificial tubular fluid perfusate	Change in TGF responses %	Change in [^{3}H]-L-arginine uptake %
Vehicle	0 ± 0 (N = 10)	+2 ± 3 (N = 10)
L-NMA (10^{-3} M)	+22 ± 4[a] (N = 5)	−43 ± 7[a] (N = 5)
ADMA (10^{-3} M)	+28 ± 3[a] (N = 7)	−32 ± 8[a] (N = 10)
SDMA (10^{-3} M)	+1 ± 2 (N = 6)	−29 ± 6[a] (N = 12)

Mean ± SEM values from renal micropuncture and microperfusion studies in which vehicle or drugs were added to artificial tubular fluid perfused from the late proximal tubule.
[a] Compared to vehicle, $P < 0.001$

lated cells of the cortical collecting ducts inhibits H^+-ATPase [13]. DDAH could be of importance in regulating NOS activity at this site and might thereby regulate proton secretion.

In conclusion, DDAH is colocalized with NOS in many cells in the kidney. Whereas L-NMA and ADMA, but not SDMA, enhance TGF responses when microperfused into the macula densa, ADMA, SDMA, and L-NMA all impair [^{3}H]-L-arginine uptake from tubular fluid of the perfused loop of Henle. These immunocytochemical and functional data suggest that the different methylarginines formed endogenously within the kidney might have complex effects on NO generation. L-NMA and ADMA appear to inhibit NOS in the JGA, whereas L-NMA, ADMA, and SDMA inhibit epithelial uptake of L-arginine from tubular fluid in the loop of Henle. The contrasting effects of ADMA and SDMA on the inhibition of NOS and on arginine transport should provide valuable investigative tools to differentiate the roles of these two processes in NO generation.

ACKNOWLEDGMENTS

This work was supported by grants from the NIDDK to CSW (DK36079 and DK49870) and by the George E. Schreiner Chair of Nephrology.

Reprint requests to Akihiro Tojo, M.D., The Second Department of Internal Medicine, University of Tokyo, 7-3-1 Hongo, Bunkyo-ku, Tokyo, Japan.
E-mail: tojyo-2im@h.u-tokyo.ac.jp

APPENDIX

Abbreviations used in this article are: L-NMA, N^G-monomethylarginine; ADMA, asymmetric N^G, N^G-dimethylarginine; NO, nitric oxide; NOS, NO synthase; DDAH, N^G, N^G-dimethylarginine dimethylaminohydrolase; DMA, dimethylarginines; nNOS, neuronal NOS; MD, macula densa; eNOS, endothelial NOS; EC, endothelial cells; iNOS, inducible NOS; PT, proximal tubules; DT, distal tubules; EDT, early distal tubules; TAL, thick ascending limbs of Henle; IC, intercalated cells of the collecting duct; CCD, cortical collecting duct; EM, electron microscopic; TGF, tubuloglomerular feedback; ATF, artificial tubular fluid; PSF, proximal stop flow pressure; SDMA, symmetric dimethylarginine; ADMA, asymmetric dimethylarginine.

REFERENCES

1. VALLANCE P, LEONE A, CALVER A, COLLIER J, MONCADA S: Accumulation of an endogenous inhibitor of nitric oxide synthesis in chronic renal failure. *Lancet* 339:572–575, 1992
2. KAKIMOTO Y, AKAZAWA S: Isolation and identification of N^G,N^G- and N^G,N'^G-dimethylarginine, N^ϵ-mono-, di-, and trimethyllysine, and

glucosylgalactosyl- and galactosyl-δ-hydroxylysine from human urine. *J Biol Chem* 245:5751–5758, 1970
3. MACALLISTER RJ, WHITLEY GSJ, VALLANCE P: Effects of guanidino and uremic compounds on nitric oxide pathways. *Kidney Int* 45:737–742, 1994
4. MACALLISTER RJ, FICKLING SA, WHITLEY GSJ, VALLANCE P: Metabolism of methylarginines by human vasculature: Implications for the regulation of nitric oxide synthesis. *Br J Pharmacol* 112:43–48, 1994
5. FICKLING S, LEONE A, NUSSEY S, VALLANCE P, WHITLEY G: Synthesis of N^G-N^G-dimethylarginine by human endothelial cells. *Endothelium* 1:137–140, 1993
6. FARACI FM, BRIAN JE JR, HEISTAD DD: Response of cerebral blood vessels to an endogenous inhibitor of nitric oxide synthase. *Am J Physiol* 269:H1522–H1527, 1995
7. KIMOTO M, TSUJI H, OGAWA T, SASAOKA K: Detection of N^G,N^G-dimethylarginine dimethylaminohydrolase in the nitric oxide-generating systems of rats using monoclonal antibody. *Arch Biochem Biophys* 300:657–662, 1993
8. KIMOTO M, WHITLEY GSJ, TSUJI H, OGAWA T: Detection of N^G,N^G-dimethylarginine dimethylaminohydrolase in human tissue using a monoclonal antibody. *J Biochem* 117:237–238, 1995
9. WILCOX CS, WELCH WJ, MURAD F, GROSS SS, TAYLOR G, LEVI R, SCHMIDT HHHW: Nitric oxide synthase in macula densa regulates glomerular capillary pressure. *Proc Natl Acad Sci USA* 89:11993–11997, 1992
10. MUNDEL P, BACHMANN S, BADER M, FISCHER A, KUMMER W, MAYER B, KRIZ W: Expression of nitric oxide synthase in kidney macula densa cells. *Kidney Int* 42:1017–1019, 1992
11. TOJO A, GROSS SS, ZHANG L, TISHER CC, SCHMIDT HHHW, WILCOX CS, MADSEN KM: Immunocytochemical localization of distinct isoforms of nitric oxide synthase in the juxtaglomerular apparatus of normal rat kidney. *J Am Soc Nephrol* 4:1438–1447, 1994
12. UJIIE K, YUEN J, HOGARTH L, DANZIGER R, STAR RA: Localization and regulation of endothelial NO synthase mRNA expression in rat kidney. *Am J Physiol* 267:F296–F302, 1994
13. TOJO A, GUZMAN NJ, GARG LC, TISHER CC, MADSEN KM: Nitric oxide inhibits bafilomycin-sensitive H^+-ATPase activity in rat cortical collecting duct. *Am J Physiol* 267:F509–F515, 1994
14. AHN KY, MOHAUPT MG, MADSEN KM, KONE BC: In situ hybridization localization of mRNA encoding inducible nitric oxide synthase in rat kidney. *Am J Physiol* 267:F748–F757, 1994
15. BACHMANN S, BOSSE HM, MUNDEL P: Topography of nitric oxide synthesis by localizing constitutive NO synthases in mammalian kidney. *Am J Physiol* 268:F885–F898, 1995
16. TERADA Y, TOMITA K, NONOGUCHI H, MARUMO F: Polymerase chain reaction localization of constitutive nitric oxide synthase and soluble guanylate cyclase messenger RNAs in microdissected rat nephron segments. *J Clin Invest* 90:659–665, 1992
17. BOSSE HM, BÖHM R, RESCH S, BACHMANN S: Parallel regulation of constitutive NO synthase and renin at JGA of rat kidney under various stimuli. *Am J Physiol* 269:F793–F805, 1995
18. TAKANOHASHI A, TOJO A, KOBAYASHI N, YAGI S, MATSUOKA H: Effect of trichlormethiazide and captopril on nitric oxide synthase activity in the kidney of deoxycorticosterone acetate-salt hypertensive rats. *Jpn Heart J* 37:251–259, 1996
19. MOHAUPT MG, ELZIE JL, AHN KY, CLAPP WL, WILCOX CS, KONE BC: Differential expression and induction of mRNA encoding two inducible nitric oxide synthase in rat kidney. *Kidney Int* 46:653–665, 1994
20. ZATZ R, DE NUCCI G: Effects of acute nitric oxide inhibition on rat glomerular microcirculation. *Am J Physiol* 261:F360–F363, 1991
21. MATTSON DL, ROMAN RJ, COWLEY AW: Role of nitric oxide in renal papillary blood flow and sodium excretion. *Hypertension* 19:766–769, 1992
22. MATSUOKA H, ITOH S, KIMOTO M, KOHNO K, TAMAI T, WADA Y, YASUKAWA H, IWAMI G, OKUDA S, IMAIZUMI T: Asymmetrical dimethylarginine, an endogenous nitric oxide synthase inhibitor, in experimental hypertension. *Hypertens* 29:242–247, 1997
23. BRIGGS JP, SCHNERMANN J: The tubuloglomerular feedback mechanism, in *Hypertension: Pathophysiology, Diagnosis and Management*, edited by LARAGH JH, BRENNER BM, New York, Raven Press Ltd, 1990, pp 1067
24. WILCOX CS, WELCH WJ: TGF and nitric oxide: Effects of salt intake and salt-sensitive hypertension. *Kidney Int* 49(Suppl 55):S9–S13, 1996
25. WILCOX CS, WELCH WJ: Effect of salt intake and y^+ transport on blunting of tubuloglomerular feedback by arginine. (abstract) *FASEB J* A546, 1996
26. BOGLE RG, MACALLISTER RJ, WHITLEY GSJ, VALLANCE P: Induction of N^G-monomethyl-L-arginine uptake: A mechanism for differential inhibition of NO synthases? *Am J Physiol* 269:C750–C756, 1995
27. TOJO A, MADSEN KM, WILCOX CS: Expression of immunoreactive nitric oxide synthase isoforms in rat kidney: Effects of dietary salt and losartan. *Jpn Heart J* 36:389–398, 1995
28. OGAWA T, KIMOTO M, SASAOKA K: Purification and properties of a new enzyme, N^G,N^G-dimethylarginine dimethylaminohydrolase, from rat kidney. *J Biol Chem* 264:10205–10209, 1989
29. SCHÖNFELDER G, JOHN M, HOPP H, FUHR N, VAN DEN GIET M, PAUL M: Expression of inducible nitric oxide synthase in placenta of women with gestational diabetes. *FASEB J* 10:777–784, 1996
30. HIRATA Y, HAYAKAWA H, KAKOKI M, TOJO A, SUZUKI E, KIMURA K, GOTO A, KIKUCHI K, NAGANO T, HIROBE M, OMATA T: Nitric oxide release from kidneys of hypertensive rats treated with imidapril. *Hypertension* 27:672–678, 1996
31. WELCH WJ, WILCOX CS: Potentiation of tubuloglomerular feedback in the rat by thromboxane mimetic. Role of macula densa. *J Clin Invest* 89:1857–1865, 1992
32. DE NICOLA L, BLANTZ RC, GABBAI FB: Nitric oxide and angiotensin II. *J Clin Invest* 89:1248–1256, 1992
33. ROCZNIAK A, BURNS KD: Nitric oxide stimulates guanylate cyclase and regulates sodium transport in rabbit proximal tubule. *Am J Physiol* 270:F106–F115, 1996
34. GUZMAN NJ, FANG M, TANG S, INGELFINGER JR, GARG LC: Autocrine inhibition of Na^+/K^+-ATPase by nitric oxide in mouse proximal tubule epithelial cells. *J Clin Invest* 95:2083–2088, 1995
35. FÖRSTERMANN U, GATH I, SCHWARZ P, CLOSS EI, KLEINERT H: Isoforms of nitric oxide synthase: Properties, cellular distribution and expressional control. *Biochem Pharmacol* 50:1321–1332, 1995
36. TRACEY WR, POLLOCK JS, MURAD F, NAKANE M, FÖRSTERMANN U: Identification of type III (endothelial-like) particulate nitric oxide synthase in LLC-PK_1 kidney tubular epithelial cells. *Am J Physiol* 266:C22–C26, 1994
37. AMOAH-APRAKU B, CHANDLER LJ, HARRISON JK, TANG S, INGELFINGER JR, GUZMAN NJ: NF-κB and transcriptional control of renal epithelial-inducible nitric oxide synthase. *Kidney Int* 48:674–682, 1995
38. SHULTZ PJ, TAYEH MA, MARLETTA MA, RAIJ L: Synthesis and action of nitric oxide in rat glomerular mesangial cells. *Am J Physiol* 261:F600–F606, 1991
39. MARKEWITZ BA, MICHAEL JR, KOHAN DE: Cytokine-induced expression of a nitric oxide synthase in rat renal tubule cells. *J Clin Invest* 91:2138–2143, 1993
40. MOHAUPT MG, SCHWÖBEL J, ELZIE JL, KANNAN GS, KONE BC: Cytokines activate inducible nitric oxide synthase gene transcription in inner medullary collecting duct cells. *Am J Physiol* 268:F770–F777, 1995
41. BAYDOUN AR, MANN GE: Selective targeting of nitric oxide synthase inhibitors to system y^+ in activated macrophages. *Biochem Biophys Res Comm* 200:726–731, 1994
42. SCHMIDT K, LIST BM, KLATT P, MAYER B: Characterization of neuronal amino acid transporters: Uptake of nitric oxide synthase inhibitors and implication for their biological effects. *J Neurochem* 64:1469–1475, 1995
43. DANTZLER WH, SILBERNAGL S: Basic amino acid transport in renal papilla: Microperfusion of Henle's loops and vasa recta. *Am J Physiol* 265:F830–F838, 1993
44. BODE-BÖGER SM, BÖGER RH, KIENKE S, JUNKER W, FRÖLICH JC: Elevated L-arginine/dimethylarginine ratio contributes to enhanced systemic NO production by dietary L-arginine in hypercholesterolemic rabbits. *Biochem Biophys Res Comm* 219:598–603, 1996